The Plastic Pathfinder: A Macroplastic Transport and Fate Model for Terrestrial Environments

Y. Mellink[a,b], T. van Emmerik[a], M. Kooi[c], C. Laufkötter[d,e], and H. Niemann[f,b,g]

[a] Hydrology and Quantitative Water Management Group, Wageningen University, Wageningen, the Netherlands

[b] Department of Earth Sciences, Faculty of Geosciences, Utrecht University, Utrecht, the Netherlands

[c] Aquatic Ecology and Water Quality Group, Wageningen University, Wageningen, the Netherlands

[d] Climate and Environmental Physics, Physics Institute, University of Bern, Bern, Switzerland

[e] Oeschger Centre for Climate Change Research, University of Bern, Bern, Switzerland

[f] Department of Marine Microbiology and Biogeochemistry, NIOZ Royal Netherlands Institute for Sea Research, 't Horntje, the Netherlands

[g] CAGE - Centre for Arctic Gas Hydrate, Environment and Climate, Department of Geosciences, UiT The Arctic University of Norway, Tromsø, Norway

Corresponding author: Y. Mellink (mellinkyvette@gmail.com)

The Plastic Pathfinder: A Macroplastic Transport and Fate Model for Terrestrial Environments

Y. Mellink[a,b], T. van Emmerik[a], M. Kooi[c], C. Laufkötter[d,e], and H. Niemann[f,b,g]

[a] Hydrology and Quantitative Water Management Group, Wageningen University, Wageningen, the Netherlands

[b] Department of Earth Sciences, Faculty of Geosciences, Utrecht University, Utrecht, the Netherlands

[c] Aquatic Ecology and Water Quality Group, Wageningen University, Wageningen, the Netherlands

[d] Climate and Environmental Physics, Physics Institute, University of Bern, Bern, Switzerland

[e] Oeschger Centre for Climate Change Research, University of Bern, Bern, Switzerland

[f] Department of Marine Microbiology and Biogeochemistry, NIOZ Royal Netherlands Institute for Sea Research, 't Horntje, the Netherlands

[g] CAGE - Centre for Arctic Gas Hydrate, Environment and Climate, Department of Geosciences, UiT The Arctic University of Norway, Tromsø, Norway

Corresponding author: Y. Mellink (mellinkyvette@gmail.com)

Abstract

Land-based plastic waste is the major source for freshwater and marine plastic pollution. Yet, the transport pathways over land remain highly uncertain. Here, we introduce a new conceptual model to forecast plastic transport on land: the *Plastic Pathfinder*; a numerical model that simulates the spatiotemporal distribution of macroplastic (>0.5 cm) at a river basin scale. The plastic transport driving forces are wind and surface runoff, while plastic transport is resisted by terrain surface friction. The terrain surface friction, a function of the slope and land use, is converted into thresholds that define the critical wind and surface runoff conditions required to mobilise and transport macroplastic waste. When the wind and/or surface runoff conditions exceed their respective thresholds, the model simulates the transport and (re)distribution of plastics, resulting in plastic accumulation hotspots maps and high probability transport route maps. The Plastic Pathfinder contributes to a better mechanistic understanding of plastic transport through terrestrial environments, and upon future calibration and validation, can serve as a practical tool to optimise plastic waste prevention, mitigation, and reduction strategies.

Abbreviations

MPW	mismanaged plastic waste
W	wind speed (m/s)
W_{thres}	wind speed threshold for macroplastic mobilisation and transport (m/s)
SR	surface runoff (mm/d)
SR_{thres}	surface runoff threshold for macroplastic mobilisation and transport (mm/d)

1. Introduction

Plastic pollution causes harm to wildlife, through ingestion or entanglement (Sigler, 2014)). Human health and livelihood in general is threatened as well, directly through for example the consumption of contaminated seafood (Ribeiro et al., 2014; ShiChun et al., 2019; Vethaak and Leslie, 2016). But also indirectly, for example the increased flood risk in urban areas due to plastic waste clogging the drains (Njeru, 2006; van Emmerik and Schwarz, 2020). Furthermore, economic activities feel negative effects as well, for example when plastic debris damages vessels or when heavily polluted beaches repel tourists. When high production rates and extensive usage of plastics exceed the capacity of the (local) waste management systems, when waste is leaking from dumps or open uncontrolled landfills, or when waste is littered, we refer to it as mismanaged plastic waste (MPW) (Geyer et al., 2017). Each year vast amounts of MPW with a land-based source enter the natural environment, where it is transported across terrestrial systems by aeolian and aquatic processes (Lebreton et al., 2017; Schmidt et al., 2017; Barboza et al., 2019; van Emmerik et al., 2019; Materić et al., 2020). It is assumed that MPW generated on land is the main source of riverine and marine plastic pollution (Biermann et al., 2020; Lau et al., 2020; Wayman and Niemann, 2021). However, several studies suggest that a fraction of the MPW is retained in terrestrial and freshwater systems (Tramoy et al., 2020; van Emmerik et al., 2022). Plastic transport and emission models have been developed over the past years to make an estimate on the amount of MPW that is emitted to the oceans via river emissions (Lebreton et al., 2017; Schmidt et al., 2017). These models use estimates of the MPW generation within a river basin and, combined with waste management, population and hydrological related variables, predict the fraction of MPW that is emitted to the ocean at the river mouth. In other words, they look at what comes in and predict what comes out, but do not take any overland transport and accumulation processes into account. Meijer et al. (2021) was the first to examine in more detail what happens in between the MPW production on land and the emission to the ocean. Their modelling study produces transport probability maps, which indicate for each location in the river basin the probability that MPW produced at that location would be emitted into the oceans within one year. By applying their model to hundreds of rivers globally, Meijer et al. (2021) estimate that less than 2% of the land-based MPW annually produced within river basins is emitted to the oceans. While their study offers valuable insights into the probability of plastic transport through river basins, the exact transport routes and accumulation hotspots of the remaining 98% remain unknown.

As of today, there are no plastic transport models that simulate the trajectories of MPW between these terrestrial compartments (Wayman and Niemann, 2021), whereas such models have already been successfully developed for the marine environment (Lebreton et al., 2012; Maximenko et al., 2012; van Sebille et al., 2012; Hardesty et al., 2017; Delandmeter and van Sebille, 2019; Onink et al., 2021). Therefore, we developed the *Plastic Pathfinder*, a macroplastic transport and fate model that simulates the pathways and spatiotemporal distribution of MPW within the terrestrial parts of river basins. The model concept is based on the assumption that macroplastic waste is

mobilised and transported when the driving forces, in this case wind and surface runoff, overcome the terrain friction caused by the (combination of the) terrain slope and type of land use. Our model additionally identifies where terrestrial pollution enters freshwater systems, which makes it valuable for the coupling with existing freshwater plastic transport models. In this paper, we introduce the basic concepts of the Plastic Pathfinder and demonstrate its use through application to an idealized case study. Besides the significant contribution to a better fundamental understanding of plastic transport and accumulation in terrestrial systems, the Plastic Pathfinder is a useful tool for developing and improving (inter)national plastic monitoring, collection and mitigation strategies.

2. Material and Methods

The model is written in Python 3.8.3 in the Jupyter Notebook (Version 6.0.3) environment, a package from Anaconda Navigator (Anaconda Software Distribution, 2016). The code of the Plastic Pathfinder and the user's manual are available at https://doi.org/10.5281/zenodo.6470410. Below, we introduce the model concept, framework, input, and output. In addition, we present an idealized case study for which we used real-world forcing input data. This model application is meant to illustrate the performances of the Plastic Pathfinder for a simple hypothetical river basin ('a proof of principle').

2.1 Model Concept

The model concept is based on a principal criterion in the field of sedimentology, which states that sediment motion is initiated when driving forces overcome resistive forces (Shields, 1936). We assume that the motion of macroplastics over land is a function of driving and resistive forces as well and that thresholds mark the conditions required for incipient motion (Fig. 1). The two driving forces in the model are wind (W) and surface runoff (SR) (the same driving forces were used by Meijer et al. (2021)) and the resisting force, i.e. the terrain friction, is a result of the combination of land use and terrain slope, which is translated to a wind (W_{thres}) and a surface runoff threshold (SR_{thres}). For each geographic location in the river basin, the wind speed (W) and surface runoff flux (SR) are compared with their respective thresholds. This comparison has four possible outcomes:

$$
\left\{
\begin{array}{llll}
W < W_{thres} & \wedge & SR < SR_{thres} & \quad (1) \\
W \geq W_{thres} & \wedge & SR < SR_{thres} & \quad (2) \\
W < W_{thres} & \wedge & SR \geq SR_{thres} & \quad (3) \\
W \geq W_{thres} & \wedge & SR \geq SR_{thres} & \quad (4)
\end{array}
\right.
$$

In case none of the thresholds are surpassed (eq. 1), the macroplastics will not be mobilised and no transport occurs. If only the wind threshold is surpassed (eq. 2), the macroplastics will move in the direction of the wind flow at that geographic location. In case only the surface runoff threshold is surpassed (eq. 3), the macroplastics will move in the direction of the surface runoff, which is equal to the direction of the steepest downhill terrain slope at that geographic location. Last, if both thresholds are surpassed (eq. 4), the model randomly picks either the wind or the surface runoff direction as the macroplastic transport direction. The reason for this randomized approach is that no data exists on how to model the relative importance of surface runoff versus wind speed. For example, it is unclear how much surface runoff is required to counteract a certain wind speed. Empirical, future experiments will be necessary to determine the combined effect of wind speed and surface runoff on the net transport (speed and direction) of macroplastics. Consequently, the two plastic transport vectors cannot be combined constructively or destructively as a simple vector product.
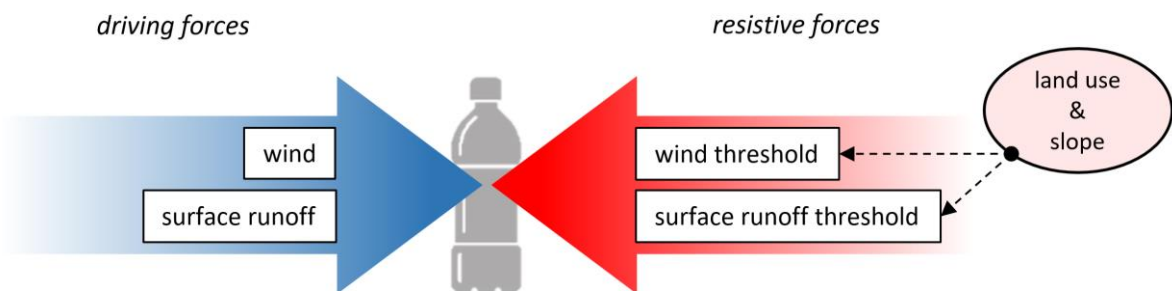

Fig. 1. Schematic representation of the main model concept of the Plastic Pathfinder. The forces that rive plastic transport are wind and surface runoff, the resistive forces are induced by the land use and slope of the terrain, which are translated to thresholds. Plastics mobilisation and transport only occurs when the driving forces exceed the resistive forces.

2.2 Model Framework

The Plastic Pathfinder requires terrain characteristics (including topography and land use), weather conditions (including wind speed/direction and surface runoff), and MPW generation (calculated from population data) (Fig. 2). The terrain characteristics in each grid cell of the model domain are translated to a plastic mobilisation and transport threshold (one threshold for wind driven transport and one threshold for surface runoff driven transport). Subsequently, the wind speed and surface runoff thresholds are compared with the wind speed and surface runoff, respectively (i.e. the weather conditions). The outcome of this comparison, presented in a plastic mobilisation map, is combined with the wind and surface runoff directions in order to simulate the transport pathways and accumulation zones of plastic waste.

2.3 Model Resolution

The model is built on a rectangular [longitude, latitude] grid, with equally sized grid cells. Input data values, i.e. grid cell properties (e.g. elevation, land use, wind, and rain), are assigned to each grid cell and assumed to be

representative for the entire area of land covered by that grid cell. The Plastic Pathfinder can operate on any desired spatial or temporal resolution depending on the required degree of detail and resolution. In our model application, we use a model domain of 30 by 30 arc seconds, a 3 by 3 arc seconds resolution (i.e. 10 by 10 grid cells), a modelled period of one year and a temporal resolution of 1 day.
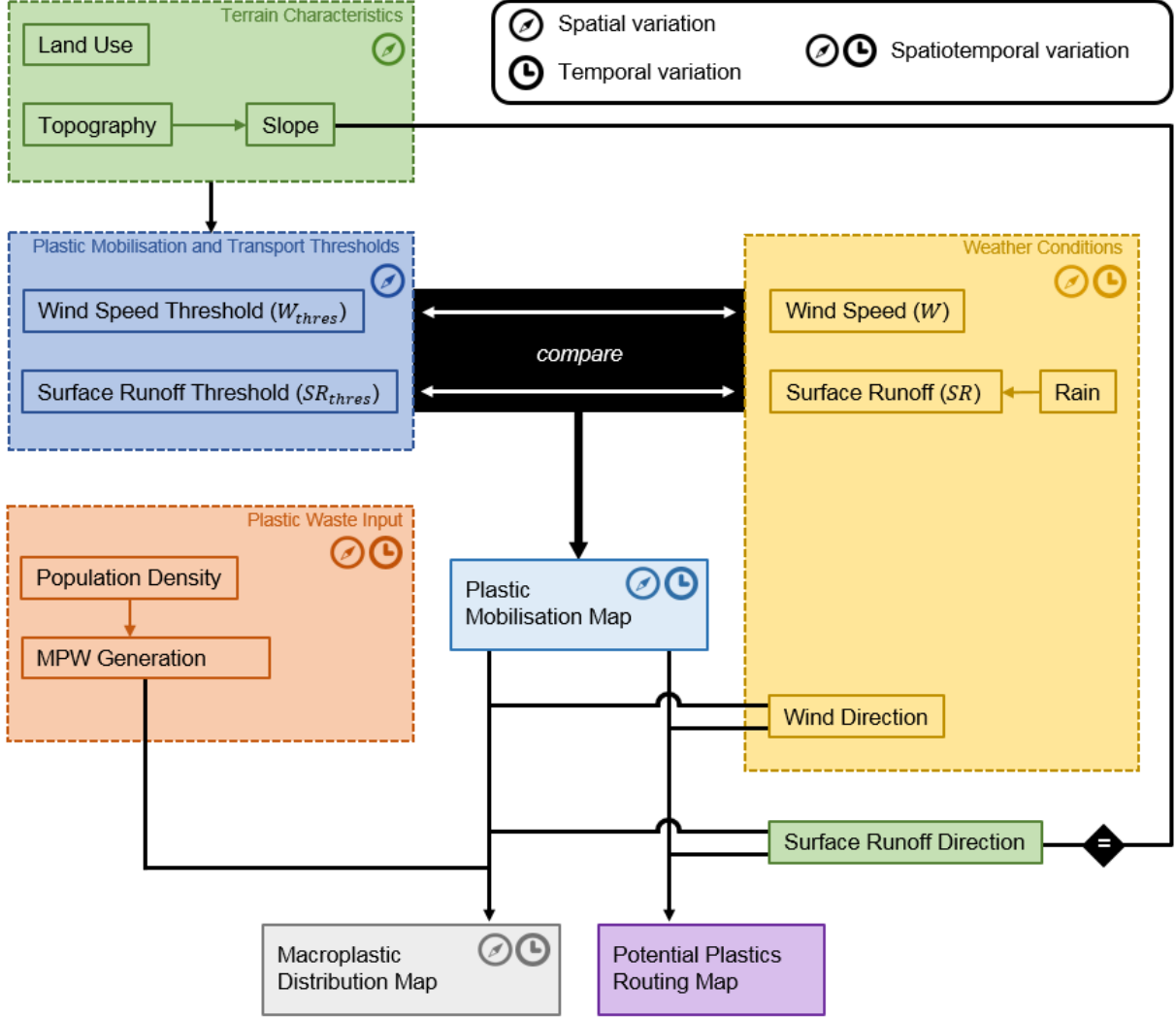

Fig. 2. Model framework of the Plastic Pathfinder. The terrain characteristics only vary in space, whereas the weather conditions and the plastic waste generation (can) vary in space and time. The surface runoff direction is equal to the steepest downhill slope direction, which is derived from the topography data.

2.4 Modelled Directions of Motion

All motions modelled by the Plastic Pathfinder occur in the two-dimensional horizontal plane. Analogous to the approach of Jenson and Domingue (Jenson and Domingue, 1988), the modelled components, i.e. air (wind), water (surface runoff) and plastics, can only move from a given grid cell to a neighbouring grid cell. As the model uses a rectangular grid, motion is restricted to eight directions: north, northeast, east, southeast, south, southwest, west and northwest. The fact that the travel distance to diagonal grid cells (i.e. towards the cells in the northeast, southeast, southwest and northwest) is longer than the travel distance to perpendicular grid cells (i.e. towards the

cells in the north, east, south and west), is accounted for in the design of the thresholds that control the displacement of plastic waste.

2.5 Model Input

2.5.1 Topography

The topography input defines for each grid cell the elevation above sea level in meters. For each grid cell the distance weight drop towards each of its neighbouring grid cells is calculated (topography data can be extracted from a database such as HydroSHEDS (Lehner et al., 2008). The model calculates the distance weighted drop in all eight directions and marks the smallest as the direction of the steepest downhill terrain slope. In case a grid cell is surrounded by grid cells with a higher topography, the smallest distance weighted drop marks the direction of the gentlest uphill slope. The fictional topography map created for the model application and the corresponding steepest downhill slope values (in meter/meter) and directions are shown in Fig 3 a and b, respectively.

2.5.2 Land Use

The land use input defines for each grid cell the type of land use. Land use data can be extracted from a database such as the ESA CCI Land Cover time-series (ESA. Land Cover CCI Product User Guide Version 2.0). The Plastic Pathfinder distinguishes between water and five types of land use:

- urban land (artificial surfaces, e.g. cities)
- bare land (little or no vegetation)
- grass/shrub land (grass and/or shrub cover, e.g. pastures)
- agricultural land (edible plants vegetation, e.g. croplands)
- forest (dense vegetation with trees, ranging from tropical rainforests to boreal forests)

These land use categories were selected on the basis of the global Land Cover Themes from the GLC2000 data set (Bartholomé and Belward, 2005). The fictional land use map created for the model application is shown in Fig. 3c. The fictional river drains towards a fictional sea in the south and the bare land grid cells (latitude 0) represents a coastline.

2.5.3 Wind Speed and Wind Direction

The wind input provides for each time step for a given grid cell the daily averaged wind speed in meters per second and the average wind direction (N, NE, E, SE, S, SW, W or NW). The wind data can be extracted from a database such as the Global Wind Atlas (Global Wind Atlas 3.0) or a local meteorological weather station. Tab. S1 was used to convert the continuous range of wind directions in degrees (0°-360°) to the eight directions of motion used in our model (see section 2.4). The wind speeds (Fig. S1) and directions (Tab. S2) used for our model application are

based on the frequency of actual wind speeds and directions measured (in the period 1981 – 2000) at the De Bilt weather station, the Netherlands (Royal Netherlands Meteorological Institute (a) and (b)) (wind speed frequency tables are provided in Tab. S3 and Tab. S4).

2.5.4 Surface Runoff

The surface runoff input provides for each time step for a given grid cell the flux of surface runoff in millimetres per day. Surface runoff data can directly be extracted from a database such as GRUN (Ghiggi et al., 2014) or computed from rainfall data using a surface runoff coefficient. The runoff coefficient (the ratio between runoff and rainfall) is the fraction of the rainwater that does not infiltrate in the soil and can transport plastics along the surface. The type of land cover (i.e. vegetation) plays a major role in this process. The surface runoff direction in each grid cell is equal to the direction of the steepest terrain slope of that grid cell (Fig. 3b). The rainfall data used for our model application (Fig. S2) is based on the frequency of actual amounts of rainfall measured between 1981 and 2000 at the De Bilt weather station, the Netherlands (Royal Netherlands Meteorological Institute (c)) (Tab. S5). We used typical runoff coefficients to convert the rainfall values into surface runoff values (Karamage et al., 2017; Goel, 2011) (Tab. S6). For our model application we assumed no time lag between a rainfall event and the generation of surface runoff. In some environments, for example in mountainous areas, a time lag between precipitation (e.g. snow) and subsequent generation of surface runoff (e.g. snow melt) is expected. In that case we recommend coupling the Plastic Pathfinder to a hydrodynamic model that takes such time lags between rainfall and the generation of surface runoff into account.

2.5.5 Mismanaged Plastic Waste Generation

The mismanaged plastic waste (MPW) input provides for each time step, for each grid cell, the mass of MPW generated in kilograms. If no MPW generation input data is available, it can be computed from the population density in combination with estimates on the (yearly) generation of solid municipal waste per capita, the fraction of waste that is mismanaged, and the proportion of plastics in solid waste (Lebreton and Andrady, 2019). The fictional population density map used for the model application indicates for each grid cell the number of inhabitants and can be found in Fig. S3. Forests were assigned an artificial population density of 0.1 people/grid cell (~12.3 people/km^2) in order to account for (occasional) littering associated to recreational activities. The yearly MPW generated in each grid cell was calculated using waste values reported for the Netherlands for the year 2015: 526 kg per capita solid waste production, of which 1% was mismanaged and 19% consisted of plastics (Lebreton and Andrady, 2019). We assumed a constant daily MPW generation and divided the yearly MPW production by 365 in order to obtain the daily MPW generation (Fig. 3d).

2.6 Plastic Mobilisation and Transport Thresholds

The Plastic Pathfinder models the mobilisation and transport of plastic waste overland on the basis of thresholds. These plastic mobilisation and transport thresholds mark the point where the driving forces overcome the resistive forces. For both transport agents, i.e. wind speed and surface runoff, we established such thresholds for the mobilisation and transport of plastics on the basis of the combination of topography and land use (Tab. 1). In general, we assumed that the plastic mobilisation and transport threshold increases with increasing terrain resistance. Below, we describe in more detail how the wind speed and surface runoff thresholds were established.
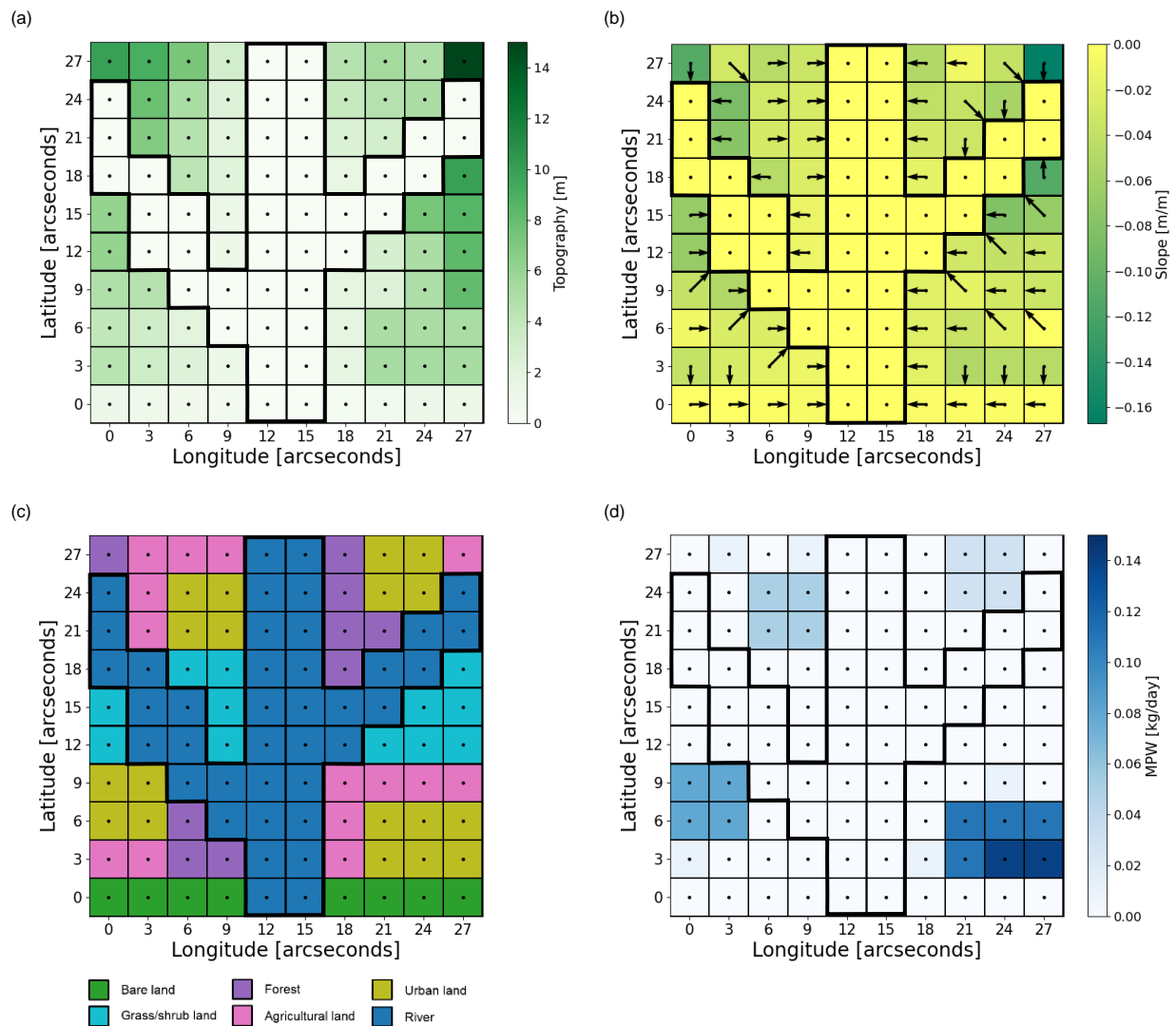

Fig. 3. (a) Topography input map used in the model application. The map shows for each grid cell the average height above sea level (m). (b) Steepest terrain slope map (calculated from the topography values). The map shows the values of the steepest slope (m/m) and the arrows indicate towards which adjacent grid cell this slope is directed. (c) Land use input map used in the model application. The map shows for each grid cell the type of land use. (d) Mismanaged plastic waste generation input map used in the model application. The map shows for each grid cell the amount of mismanaged plastic waste that is generated during each time step (kg/day). The thick black contours in all four maps indicate the boundaries of the river channel.

Tab.1. Wind speed (W_{thres}) and surface runoff threshold (SR_{thres}) values used by the Plastic Pathfinder. These values indicate for each combination of land use and terrain slope, the critical wind speed (m/s) and surface runoff (mm/d) presumed to mobilise and transport macroplastics. R_{x-y} refers to the surface runoff threshold for downhill slopes with a slope angle between x and y degrees.

|	Wind speed threshold, W_{thres}, in meters per second			Surface runoff threshold, SR_{thres}, in millimetres per day								
	Flat terrain	radian uphill[1]	radian downhill[1]	R_{0-10}	R_{10-20}	R_{20-30}	R_{30-40}	R_{40-50}	R_{50-60}	R_{60-70}	R_{70-80}	R_{80-90}
Water body	30.0	n/a	n/a	0.00	0.00	0.00	0.00	0.00	0.00	0.00	0.00	0.00
Urban land	8.8	+ 4.2	- 4.2	2.00	1.75	1.50	1.25	1.00	0.75	0.50	0.25	0.001
Bare land	6.6	+ 4.2	- 4.2	3.00	2.75	2.50	2.25	2.00	1.75	1.50	1.25	1.00
Grass/shrub land	10.0	+ 4.2	- 4.2	4.00	3.75	3.50	3.25	3.00	2.75	2.50	2.25	2.00
Agricultural land	13.2	+ 4.2	- 4.2	5.00	4.75	4.50	4.25	4.00	3.75	3.50	3.25	3.00
Forest	26.4	+ 4.2	- 4.2	7.00	6.75	6.50	6.25	6.00	5.75	5.50	5.25	5.00

2.6.1 Wind Speed Thresholds

The wind speed thresholds define the critical wind speed that is presumed to be sufficient to mobilise and transport macroplastics. The wind speed thresholds can be calculated as a function of only the type of land use (option 1) or as a function of the type of land use and the combination of terrain slope and wind direction (option 2). Below we describe both options.

Option 1: Starting point in defining the wind speed thresholds was the Beaufort wind scale, according to which a wind speed around 6.6 m/s (BF4) "*raises dust and loose paper*" (Met Office, 2010). The density of paper, 1.2 g/cm^3, is similar to the density of plastic waste. For example, plastic bottles are made from polyethylene terephthalate, which has a density of 1.37 g/cm^3 (Yeo and Hsuan, 2010), and plastic bags are made from low density polyethylene, which has a density between 0.910 and 0.925 g/cm^3 (Batra, 2014). Therefore, we established a wind speed threshold of 6.6 m/s for flat bare lands (Tab. 1). Subsequently, the value of 6.6 m/s was extrapolated in order to obtain the thresholds for the other four land use types. The extrapolation factors were derived from the overland plastic transport probabilities estimated by a panel of 24 experts in a survey conducted by Meijer et al. (2021). The averages of their estimates on the overland transport probability for 'bare land', 'urban', 'agricultural land' and 'forests', were 0.96, 0.75, 0.44, and 0.17, respectively. We roughly interpreted these averages as 1.00, 0.75, 0.50 and 0.25 (bare land, urban, agricultural land, and forests). The 6.6 m/s threshold for bare lands corresponds to the probability of 1.00. Subsequently, we established the wind speed thresholds for urban, agricultural land and forests, by multiplying 6.6 m/s with the reciprocals of 0.75, 0.50, and 0.25, respectively (Fig. 4). Since the panel of experts were not asked for the overland transport probabilities of plastics across grass/shrub lands, we assumed grass/shrub lands to have a degree of resistance in between urban and agricultural land and established a value between 8.8 m/s and 13.2 m/s: 10.0 m/s. Once plastic waste has entered a water body, e.g. a lake or a river, we assumed that only violent storms and hurricanes can lift and remove plastic waste from the water body. Therefore, a value of 30 m/s was established as wind threshold for water bodies.

Option 2: For this calculation of the wind speed threshold it was assumed that the ability of the wind force to mobilise and transport macroplastics (in the direction of the wind) decreases for uphill winds and increases for downhill winds. The reasoning behind this is that in the case of uphill winds, the wind force is counteracted, while

for downhill winds it is assisted, by the force of gravity. Therefore, apart from the land use, the topography is taken into account as well. For each radian of terrain slope angle, 4.2 m/s is added (for uphill winds) or subtracted (for downhill winds) from the wind speed thresholds that hold for flat terrains (second column in Tab. 1). The value of 4.2 m/s was determined by assuming that the wind speed threshold for (hypothetically) vertical bare lands equals 0.0 m/s (free fall). This would imply that a decrease of 6.6 m/s of the wind speed threshold, corresponds to a terrain slope increase of 90° (½π radians). For simplification, we assumed a linear relation, which translates to a decrease of 4.2 m/s for each radian of terrain slope increase. An important implication of this approach is that the wind speed thresholds do not only vary in space, but in time as well, since the wind directions can vary with time. For example, at time *t*, a certain wind speed at a specific location appears to be insufficient to mobilise and transport macroplastics, while at *t+1*, the same wind speed *but in a different direction* appears to be sufficient to surpass the wind speed threshold and consequently displaces the macroplastics.

In our model application we used option 1, i.e. the wind speed thresholds are a function of only the type of land use.
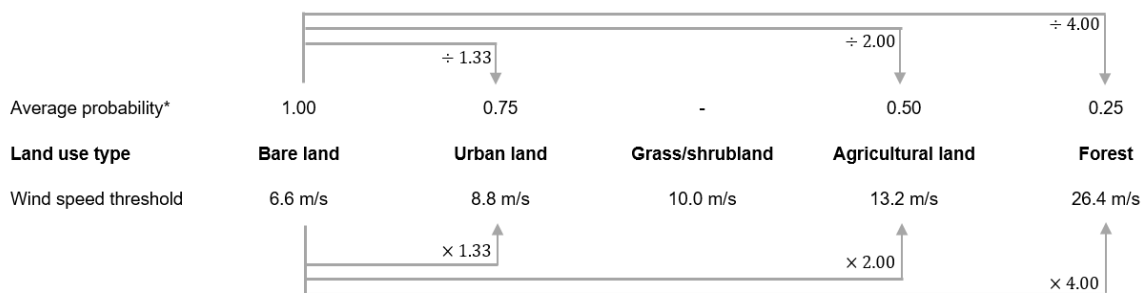
* Average of the probability estimates from a panel of experts (from Table S9 in Meijer et al. (2021))

Fig. 4. Schematic representation of the extrapolation calculation performed to obtain the wind speed thresholds. The multiplication factors at the lower arrows are the reciprocals of the average probability plastic transport estimates for four types of land use, which were estimated by a panel of experts in a survey by Meijer et al. (2021). Note that the panel of experts were not asked for the plastic transport probability of plastic across grass/shrublands. The wind speed threshold for grass/shrubland, 10 m/s, was randomly chosen between 8.8 and 13.2 m/s.

2.6.2 Surface Runoff Thresholds

The surface runoff thresholds define the critical flux of surface runoff that is presumed to be sufficient to mobilise and transport macroplastics. However, as far as we know, no study to date has examined the mobilisation and transport capacity of surface runoff. We made a first attempt and established the orders of magnitude for the surface runoff thresholds based on the distribution of data on global absolute runoff trends from the Global Runoff Reconstruction (GRUN) model, an observational-based global reconstruction of (monthly) runoff developed by Ghiggi et al. (2014). In urban areas, the smooth surface of asphalt roads and pavements are assumed to exert a low resistance force to the mobilisation and transport of plastics by surface runoff. Therefore, urban areas were assigned with the low surface runoff thresholds ranging from 0.001 mm/day for nearly vertical areas, to 2.00 mm/day for flatter areas (up to 10°) (Tab. 1). The highest resistance to plastic transport by surface runoff is thought to occur in forests, due to the vegetation that both reduces the surface runoff flow and entraps plastic waste. Therefore,

forests were assigned with the highest thresholds ranging from 5 mm/day for steep areas, to 7 mm/day flatter areas (Tab. 1). We assumed that the steeper the terrain slope, the higher the surface runoff flow velocity and the higher the capability of the surface runoff to mobilise and carry macroplastics. The terrain topography and land use are both constant through time, therefore, the surface runoff thresholds only have a spatial, and not a temporal, variability. Surface runoff driven plastic transport from grid cells that are only surrounded by higher topographies (depressions in the landscape) is assumed impossible. Consequently, plastic waste in those grid cells can only be transported away by the wind.

2.7 Macroplastic Transport

The Plastic Pathfinder works with so called *MPW clusters*, whereby a single MPW cluster consists of all the MPW that was generated in a single grid cell during a single time step. Once MPW is released from its land-based source, it is available for transport. The MPW clusters are considered to consist of different types of plastic waste (e.g. plastic bottles, bags, food wrappers), which are likely to have different mobilisation and transport behaviour. However, the mobilisation and transport thresholds of different types of plastics over land has not been studied up to date. Due to this knowledge gap we were forced to assume that all plastics have the same mobilisation and transport thresholds. Consequently, when transport is triggered, all plastic items, regardless of their type, are displaced. When different MPW clusters are transported towards the same grid cell, or when a new MPW cluster is generated in a (land) grid cell in which another MPW cluster was already present, the mass of all those MPW clusters are added. In this way MPW clusters can 'expand'.

The Plastic Pathfinder only models the transport and accumulation of plastics in terrestrial environments. When the wind or surface runoff forces MPW cluster(s) from a land into a river grid cell, the simulation of its transport ends and the plastics will remain (and fictively accumulate) in that river grid cell. The Plastic Pathfinder can be coupled to hydrological models to simulate the transport (and retention) of plastics in freshwater environments as well.

2.8 Model Output

There are three main types of output created by the Plastic Pathfinder. First of all, the wind speed and surface runoff threshold maps that show the critical wind speeds and surface runoff fluxes, respectively, which are required to mobilise and transport macroplastic. Secondly, there are the spatiotemporal MPW distribution output maps that show for each time step the amount of MPW that is present in each part of the river basin. This type of output depends on the MPW generation input data that was given to the model. The simulated (re)distribution of the MPW mass can be studied on the river basin scale or on a smaller scale, e.g. on the level of individual model grid cells. For the latter, we use the following formula de calculate the MPW stock during each time step of the model simulation:

$$MPW\ stock\ (t)_{[lon,lat]} = \left(MPW\ generation\ (t)_{[lon,lat]} + \sum_{k}^{8} MPW\ received\ (k)(t)_{[lon,lat]} \right) - MPW\ lost\ (t)_{[lon,lat]}$$

where $MPW\ stock\ (t)_{[lon,lat]}$ is the total amount of MPW (kg) present in the grid cell at latitude lat and longitude lon by the end of time step t, $MPW\ generation\ (t)_{[lon,lat]}$ is the total amount of MPW (kg) generated (e.g. littering) in the grid cell at latitude lat and longitude lon at (the start of) time step t, $MPW\ received\ (k)(t)_{[lon,lat]}$ is the amount of MPW (kg) that the grid cell at latitude lat and longitude lon received from a neighbouring grid cell k (maximum number of eight surrounding grid cells) during time step t, and $MPW\ lost\ (t)_{[lon,lat]}$ is the total amount of MPW (kg) that is transported out of the grid cell at latitude lat and longitude lon during time step t. The third type of model output is independent of the MPW generation input data and is presented in a 'potential plastic routing map'. This output focuses on the potential pathways of macroplastic waste through a river basin.

3. Results

Here, we present the spatiotemporal distributions and transport routes of MPW that we found for our model application. The modelled MPW transport and accumulation are controlled by the values chosen for the plastic mobilisation and transport thresholds (Tab. 1), which resulted in the wind speed and surface runoff threshold maps shown in Fig. S4a and S4b, respectively. We are aware of the fact that those threshold values have no emperical basis yet. Here, we merely intend to demonstrate the potential and applicability of the output of the Plastic Pathfinder model and show that this model can serve as an effective tool to examine how weather conditions can be used to predict the accumulation and transport processes of macroplastics on land.

3.1 Spatiotemporal Macroplastic Distribution

3.1.1 River Basin Scale

In our model application, we simulated the (re)distribution of a daily MPW input (Fig. 3d) for 365 days. For each time step an MPW distribution map is generated, showing the MPW stock (in kg) present in each grid cell by the end of that time step. The arrows in the MPW distribution maps show in which directions MPW was transported during that time step, whereby the thickness of the MPW transport arrow is linearly proportional to the amount (in kg) of displaced MPW. In general, during rainy days the MPW that is present in the river basin is transported in the direction of the steepest downhill slopes and during windy days the MPW get transported along with the wind. Here, we zoom in on three time steps, all of which have a different set of wind and rain conditions: day 291, 344, and 354 (Fig. 5a). On day 291 – low wind & high rain – the mobilisation map illustrates that in most grid cells the surface

runoff threshold is exceeded (Fig. 5e). In those grid cells MPW is transported in the direction of the steepest downhill slopes, i.e. the surface runoff directions (Fig. 5b and 5h). On day 344 – high wind & high rain – the mobilisation map illustrates that in the grid cells in the south of the domain both thresholds are exceeded (Fig. 5f). As a result, the MPW in those grid cells is transported either in the direction of the wind or the surface runoff (Fig. 5c and 5i) (the model randomly picks between the two). On day 354 – high wind & no rain – the mobilisation map reveals that in many grid cells the wind threshold is exceeded (Fig. 5g). Accordingly, the MPW in those grid cells is transported in the direction of the wind (Fig. 5d and 5j).

The spatiotemporal MPW distribution maps provide insights on the MPW transport and when and where MPW accumulates, how long it resides in these terrestrial accumulation zones, and under which (extreme) weather conditions it becomes (re)mobilised/(re)distributed. The Plastic Pathfinder does not simulate the transport of MPW in rivers. The advantage of this is that MPW (fictitiously) accumulates in river grid cells, which subsequently reveals where the main river entry points of MPW are located. For example, in our application the river grid cell at latitude 12 and longitude 18 is a more important entry point of MPW from land to river, than the river grid cell at latitude 21 and longitude 24 (Fig. 5h-j).

To understand terrestrial plastic pollution, knowledge on the MPW in- and output fluxes on the catchment scale is necessary. In our model, the input flux consists of the daily MPW input (Fig. 3d), and there are three ways for MPW to leave the terrestrial environment: leakage to the river, direct coastal leakage to the ocean, and leakage to adjacent land in the neighbouring watershed. Fig. 6a shows these cumulative fluxes through time for our model application, illustrating that the majority of the MPW produced on land reaches the river. This type of output provides valuable insights in the fate of MPW generated on land. Additionally, the distribution of MPW over the terrestrial and freshwater compartments of the river basin can be plotted through time (Fig. 6b). This graph shows that after ~100 days, the MPW stock on land stabilises around a value of 38 kg (STD 16 kg), which implies that the MPW produced on land approximately equals the amount of MPW lost. Please note that no removal processes in the river system were included in the model (e.g. beaching or transport to the ocean).
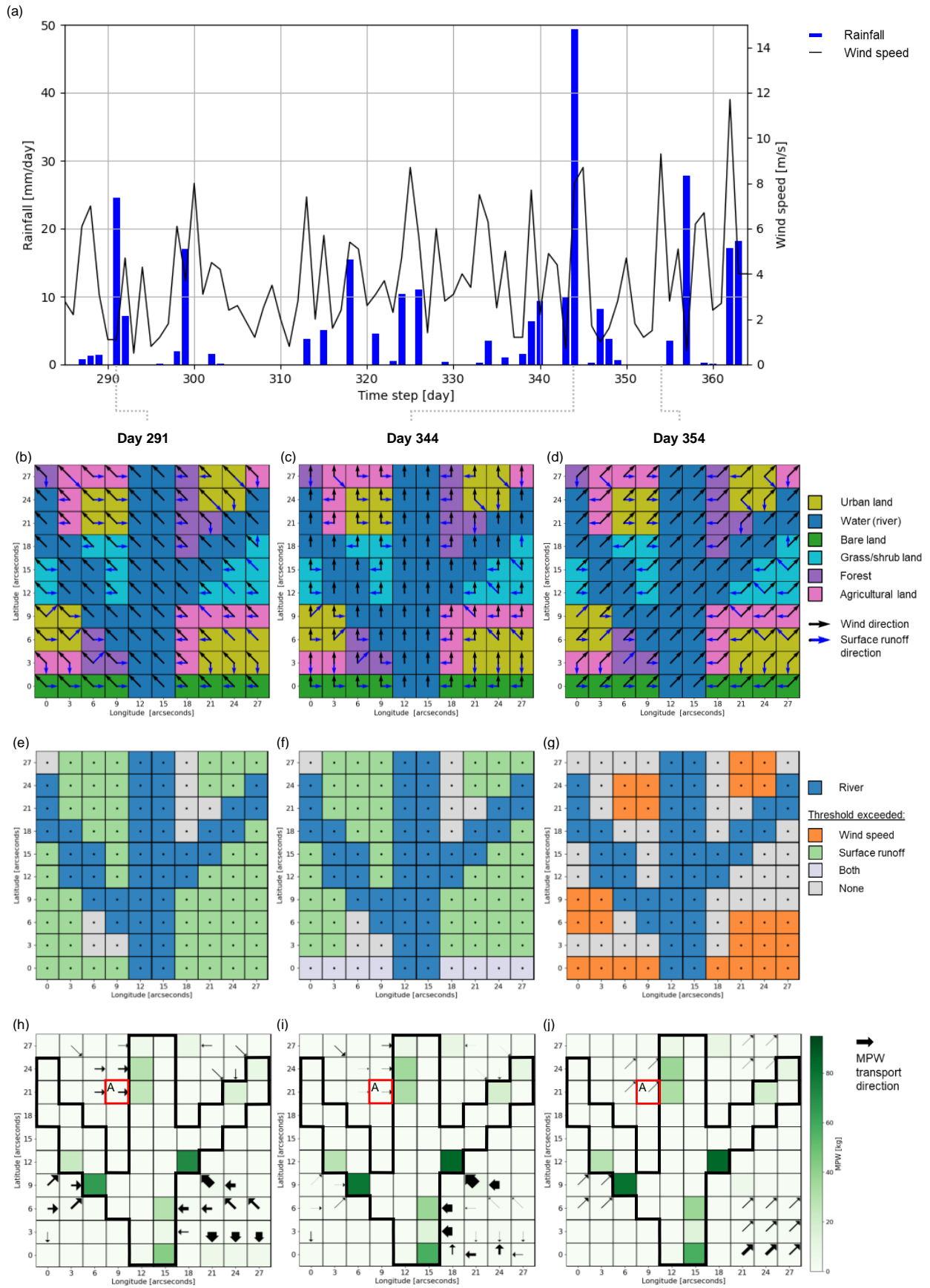
Fig. 5. (a) Rainfall and wind speeds for the time steps 285 to 364 in the model application. (b), (c), (d) Wind and surface runoff directions for the time steps 291, 344, and 354, respectively. Note how wind direction changes depending on the weather, whereas the surface runoff direction, determined by the topography, remains constant over time. (e), (f), (g) Plastic mobilisation maps for the time steps 291, 344, and 354, respectively. (h), (i), (j) Mismanaged plastic waste (MPW) distribution (kg per grid cell) maps

for the time steps 291, 344, and 354, respectively. The arrows show the MPW fluxes (kg/day) that occurred during that time step. The thickness of the arrows is linearly proportional to the magnitude of the MPW flux, i.e. the mass of MPW that was displaced during that day. The red box 'A' highlights the grid cell for which an additional local assessment of the MPW evolution has been carried out (see section 3.1.2). The thick black contours in maps e to j indicate the boundaries of the river channel.
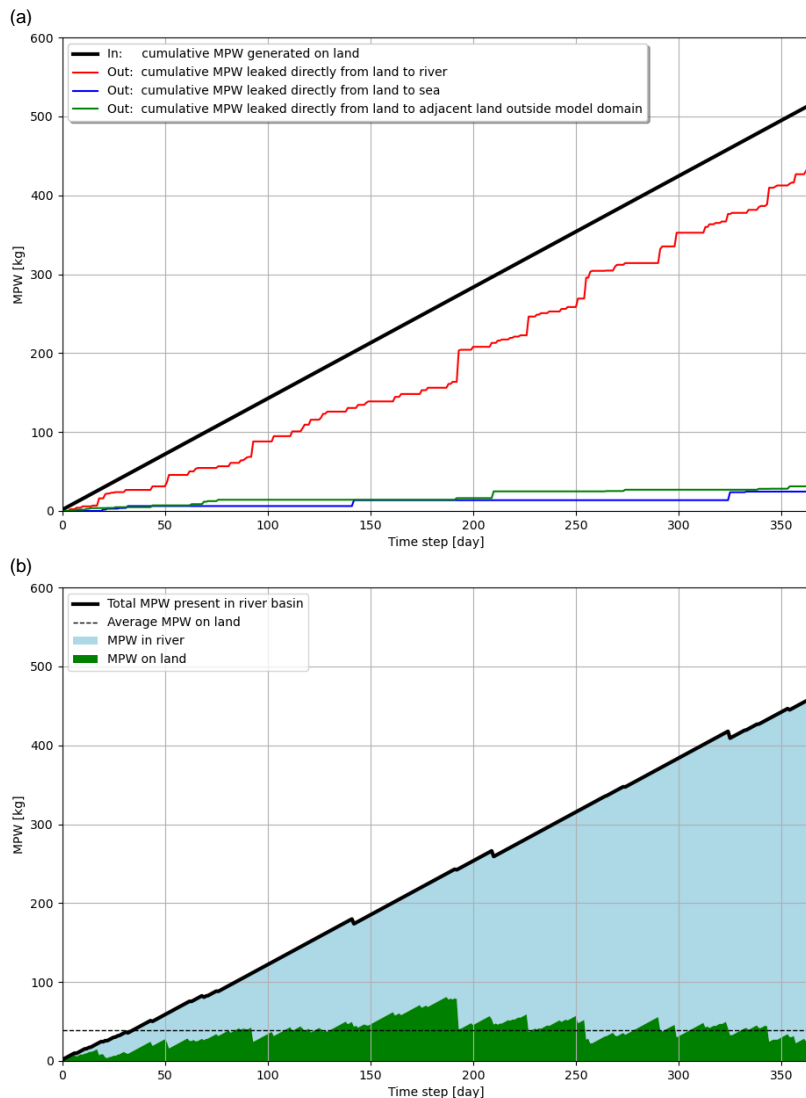
(a)

(b)

Fig. 6. (a) Cumulative in- and output fluxes of mismanaged plastic waste (kg) of the terrestrial compartment of the river basin modelled in the model application. The MPW input represents the constant daily on land MPW generation. There are three ways for MPW to leave the terrestrial domain: direct leakage into the river, direct leakage into the ocean, or direct leakage to land from an adjacent river basin. (b) The total amount of MPW (kg) present in the entire river basin, i.e. on land and in the river. The green shading represents the amount of MPW (kg) on land and the blue shading corresponds to the amount of MPW (kg) in the river. The black dashed line marks the average amount of MPW (kg) on land during the 365 time steps that were modelled in the model application.

3.1.2 Local Scale

Apart from MPW distribution assessments on a river basin scale, the MPW stock of single grid cells can be relevant

as well, for example for the design of local measures against terrestrial plastic pollution. Fig. 7a shows the MPW in-

and output of the urban grid cell located at latitude 21 and longitude 9 (indicated with 'A' in Fig. 5) for day 200 to

250. Every day this grid cell receives 0.05 kg of MPW due to in-situ MPW generation (Fig. 3d), e.g. littering and

inadequate waste collection management. For some days, e.g. 205, 225, and 248, the MPW input exceeds the

MPW output (green shading), which means a net accumulation of MPW. While for other days, e.g. 209, 227, and 247, the MPW input is lower than the MPW output (red shading); i.e., a net loss of MPW (Fig. 7a). To understand when regions net gain or lose MPW, the weather conditions on these days must be considered. For our model application we found a strong dependency between the amount of rainfall and the net loss of MPW. For example, on day 227 the amount of rainfall is 28.8 mm, and although the cell receives 0.20 kg of MPW from a neighbouring cell, it lost 0.35 kg that day due to surface runoff driven transport. We found that extreme wind speeds, on the other hand, do not necessarily result in a (net) loss of MPW, e.g. day 210 (Fig. 7a and b).
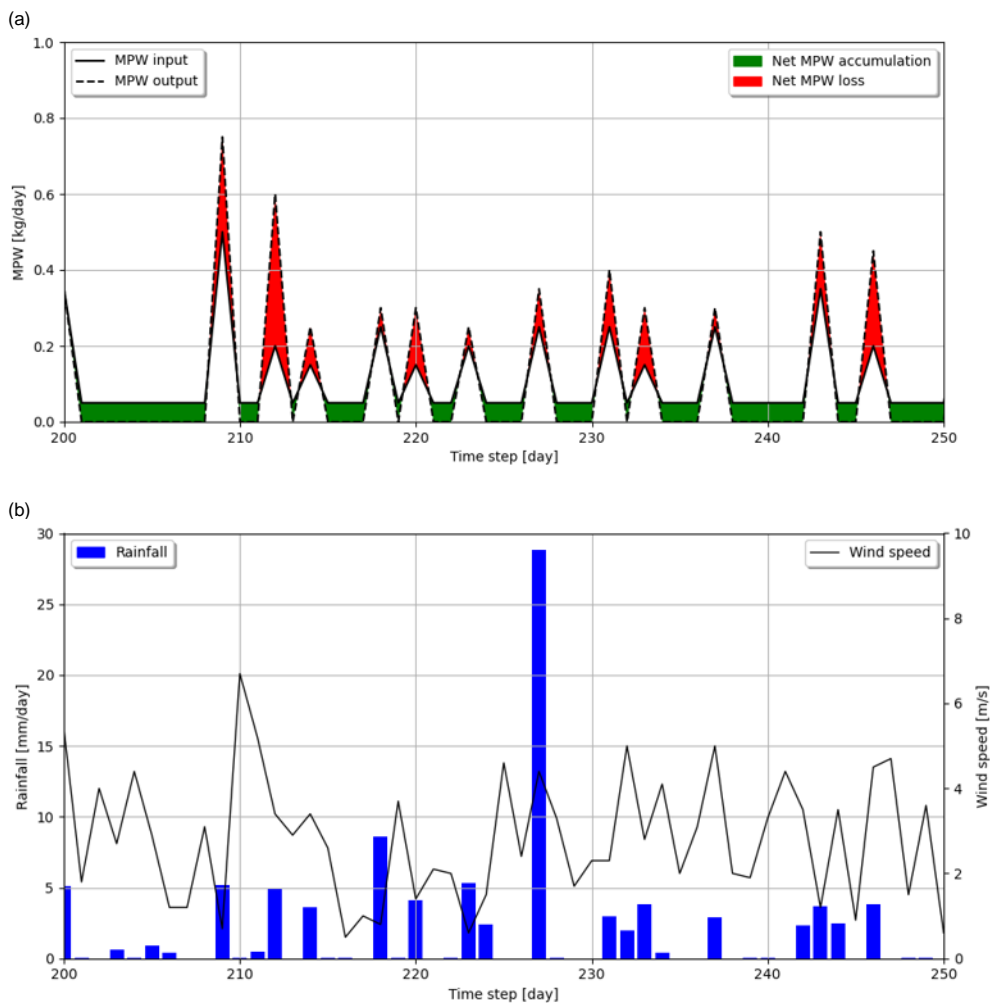

Fig. 7. (a) The in- and output fluxes of mismanaged plastic waste (kg/day) modelled for the urban grid cell at latitude 21 and longitude 9 (indicated with red box A in Fig. 5) for the period day 200 to 250 in the model application. A net accumulation of mismanaged plastic waste (green shading) occurs when the output flux exceeds the input flux. A net loss of mismanaged plastic waste (red shading) occurs when the output flux is lower than the input flux. (b) Rainfall (mm/day) and winds speeds (m/s) for the period day 200 to 250 in the model application.

3.2 Plastic Transport Routes

Apart from simulating the transport and (re)distribution of MPW that has been added to a river basin, the Plastic Pathfinder can also compute the most likely transport directions of MPW within a river basin for a given set of weather conditions. For this, the model registers for each grid cell in the river basin whether the weather conditions

trigger MPW transport, and if so, in which direction. This is done for each time step and for each grid cell, the model keeps count of how often MPW transport is forced in each of the eight transport directions (N, NE, E, SE, S, SW, W, NW). By the end of the last time step, each grid cell has obtained a transport direction distribution. These transport direction distributions are shown in a 'potential plastics routing map', whereby the width of the MPW transport arrows are linearly proportional to the frequency with which MPW transport was forced in that particular direction.

The potential plastics routing map generated by our model application (Fig. 8) demonstrates that in most grid cells, there is one dominant MPW transport direction. For example, in the grid cell at latitude 24 and longitude 21, the weather input conditions most frequently forced MPW transport to the southeast. The forest grid cells have no transport arrows, this is because the weather conditions were never sufficient to exceed either the wind or surface runoff thresholds. Logically, MPW has the highest chance to be transported in the highest frequency transport directions. Consequently, connecting the high frequency transport directions, i.e. the thickest arrows in the potential plastics routing map, provides a first order estimate on the most likely overland transport route(s) of MPW on a river basin scale.
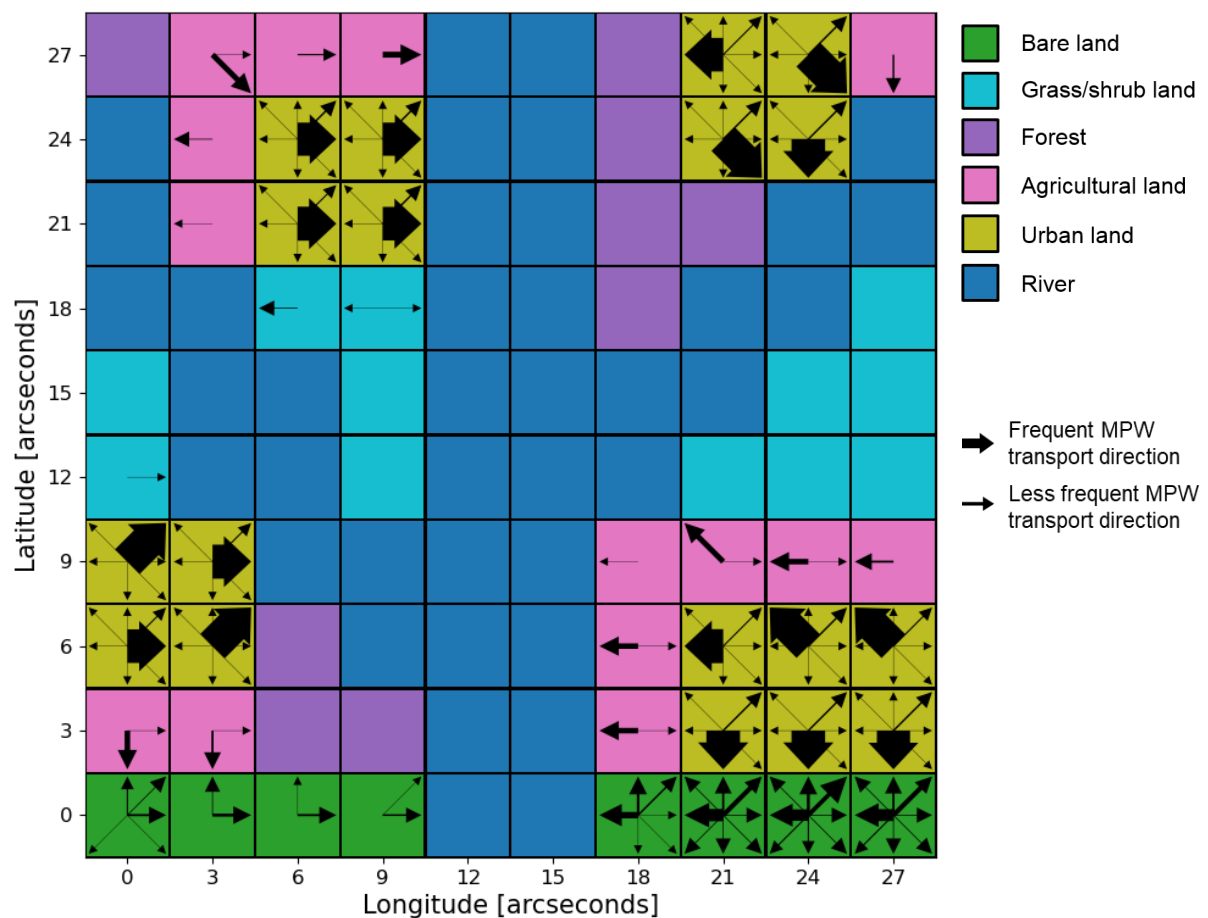

Fig. 8. Potential plastics routing map that was generated in the model application. Arrows indicate the MPW transport directions that occurred as a result the terrain characteristics, thresholds, and weather conditions used in the model application described in this study. The width of the arrow is linearly proportional to the frequency with which MPW was transported in that particular direction.

4. Discussion

4.1 The Plastic Pathfinder – an Innovative Tool

The Plastic Pathfinder is the first model to simulate the transport and accumulation of macroplastic waste over land. Without a fundamental understanding of the MPW transport and retention mechanism in terrestrial systems, the global plastic mass budget cannot be solved (Stephens, 2020; Hoellein and Rochman, 2021). Our model generates potentially high resolution MPW distribution maps, which provide insights on the mechanisms that control the (re)distribution and fate of MPW on land. Moreover, the Plastic Pathfinder identifies the main river entry points of MPW, the locations where terrestrial pollution meets freshwater pollution. With this, the input conditions for riverine plastic transport models can be fine tuned, which in turn will lead to improved estimates on riverine plastic transport, retention, and emissions to the ocean.

Alongside its scientific significance, the Plastic Pathfinder has a societal relevance as well, as it can provide guidance on the prioritisation of plastic pollution prevention, mitigation and reduction strategies. By knowing when and where plastics on land accumulate and which transport routes they take, targeted clean-up and entrapment strategies can be developed. The removal of plastics from the natural environment is a matter of great urgency, because plastic waste poses serious threats to species health and human livelihood in general (Bucci et al., 2020; Everaert et al., 2020; van Emmerik and Schwarz, 2020; Windsor et al., 2019).

4.2 Next Steps

4.2.1 Model Calibration and Validation

The Plastic Pathfinder is the first explicit spatiotemporal framework that models the transport of macroplastics in terrestrial environments. However, there are still many uncertainties associated with the accuracy of the model parameterisation, because data is scarce. The next important step is to empirically determine the mobilisation and transport thresholds. For example, physical experiments (e.g. on artificial hillslopes) can elucidate under which wind and surface runoff conditions different types of macroplastics are mobilised and transported over terrains with varying slopes and land uses. Such experiments would offer valuable insights on the mobilisation and transport thresholds of different types of plastic waste (e.g. size, shape, density, wet/dry, etc.) (Schwarz et al., 2019). Moreover, from these experiments the relation between wind speed and plastic transport speed, and surface runoff intensity and plastic transport speed can be explored. These velocities can be used to estimate the travel time of plastics through the terrestrial environment and thereby improve our estimates on the amount of land based MPW that reaches the river, and subsequently the ocean.

Once the Plastic Pathfinder contains empirically proven mobilisation and transport thresholds, the model predictions would ideally be calibrated and validated with observational data. The modelled macroplastic waste

distribution on land can be compared with actual macroplastic distribution data; quantified by e.g. field plastic collection efforts (van Emmerik et al., 2020), citizen litter collection projects (Syberg et al., 2020), or optical satellite data (Biermann et al., 2020). We anticipate that future collaborations with field collection and monitoring projects allow for a fast and robust calibration of the Plastic Pathfinder and improve the validity of its predicted MPW transport and fate in river basins.

4.2.2 Future Recommendations on the Model Concept

The plastic transport simulated by the Plastic Pathfinder is based on the concept of driving forces that need to overcome thresholds. Although this concept appears capable of providing first order predictions on the mobilisation and transport of plastics over land, we would like to make some recommendations for future research. For example, to explore the possibility of a more probabilistic modelling approach (Kooi and Koelmans, 2019), whereby the chance of plastic transport under certain weather conditions is considered, instead of all plastics either move or they don't. In addition, previous studies have shown that different types of macroplastics have different transport processes (Schwarz et al., 2019). Therefore, we recommend to use thresholds that are tailored to different types of plastics rather than assuming the same wind and surface runoff thresholds for all plastic waste.

Although the plastic mobilisation and transport thresholds provide information on *when* (i.e. under which weather conditions) plastics will move, they do not specify *how far* the plastics will be moved. In the current version of the Plastic Pathfinder the displacement of plastics is restricted to one grid cell per time step, which is acceptable as long as a positive correlation exists between the values of the thresholds and the grid resolution. Up to date, the travel distance of plastics over land has only been studied for (airborne) microplastics (Allen et al., 2019). We strongly recommend future fundamental research on the relation between wind speed and plastic transport speed and, similarly, between surface runoff fluxes and plastic transport speed.

Moreover, the spatial model resolution determines the degree of detail regarding landscape features. When the model resolution is too low, barriers that obstruct the transport of plastic waste are unjustly not taken into account. For example, the height difference of (narrow) dikes along river banks might be too small to be captured in the topography map, which uses the average height of the area that the grid cell represents. In the same way, buildings and sewage systems in urban areas or riverbank vegetation are landscape features that are too small to be captured in the land use map. We challenge future research to find a balance between small scale landscape features and covering an entire river basin in terms of spatial resolution.

Finally, we advocate for an all-encompassing model that includes the terrestrial and freshwater environment. This can be achieved by coupling thee Plastic Pathfinder with river plastic transport models. The river entry points predicted by the Plastic Pathfinder will form this link as they deliver information on where, when and how much plastic waste leaks from land into the river system. This will allow for genuine estimates on how much of the generated land-based plastic waste actually reaches the oceans via rivers.

5. Conclusions

Each day vast amounts of mismanaged plastic waste (MPW) enter the natural environment. Although various studies have examined where and when MPW is generated and emitted, the actual trajectory between land-based source and marine sink remained largely unresolved. For this reason, we developed the Plastic Pathfinder, a numerical modelling framework that simulates specific spatiotemporal distributions and trajectories of macroplastic waste resulting from wind and surface runoff driven transport on a river basin scale. Our model improves the fundamental understanding of the mobilisation, transport, (re)distribution, and accumulation patterns of macroplastics over land. The spatiotemporal plastic distribution maps can reveal the locations of terrestrial accumulation zones and reveal the main entry points of plastics from land into rivers. In addition, our model can resolve the highest probability transportation routes of plastic waste through river basins. The Plastic Pathfinder can help to locate and prioritize plastic waste monitoring locations. Moreover, it can support the development of targeted clean-up and close-to-the-source interception strategies, which could lead to both an effective removal of plastics from the terrestrial environment as well as preventing plastics from entering the freshwater and marine environment.

Authors' Contributions

Conceptualisation: YM, TvE; Methodology: YM, TvE; Software: YM; Validation: YM, TvE; Formal analysis: YM, TvE, MK, CL; Investigation: YM; Data curation: YM; Writing – original draft: YM; Writing – review & editing: YM, TvE, MK, CL, HN; Visualisation: YM; Supervision: TvE, HN; Project administration: YM; Funding acquisition: TvE. All authors read and approved the final manuscript.

Declaration of Competing Interest

The authors declare that they have no competing interests.

Availability of Data and Materials

All data used in this study are included in this published article and its Supplementary Materials. The Plastic Pathfinder is a numerical code written in Python in the open-source web application Jupyter Notebook. The Plastic Pathfinder code (.ipynb file) and the user's manual are available at https://doi.org/10.5281/zenodo.6470410.

References

Allen S, Allen D, Phoenix VR, Le Roux G, Durántez Jiménez P, Simonneau A, et al. Atmospheric transport and deposition of microplastics in a remote mountain catchment. Nat Geosci. 2019;12(5):339–44 http://dx.doi.org/10.1038/s41561-019-0335-5.

Anaconda Software Distribution. Computer software. Vers. 2-2.4.0. Anaconda. 2016. https://anaconda.com.

Barboza LGA, Cózar A, Gimenez BCG, Barros TL, Kershaw PJ, Guilhermino L. Macroplastics Pollution in the Marine Environment. In: World Seas: an Environmental Evaluation. London: Academic Press; 2019. p. 305–28. http://dx.doi.org/10.1016/B978-0-12-805052-1.00019-X.

Bartholomé E, Belward AS. GLC2000: a new approach to global land cover mapping from Earth observation data. Int J Remote Sens. 2005;26(9):1959–77 http://dx.doi.org/10.1080/01431160412331291297.

Batra K, Role of Additives in Linear Low Density Polyethylene (LLDPE) Films. 2014. p. 9. https://www.slideshare.net/kamalbatra111/polyethylene-pe

Biermann L, Clewley D, Martinez-Vicente V, Topouzelis K. Finding plastic patches in coastal waters using optical satellite data. Sci Rep. 2020;10(1):5364 http://dx.doi.org/10.1038/s41598-020-62298-z.

Bucci K, Tulio M, Rochman CM. What is known and unknown about the effects of plastic pollution: A meta-analysis and systematic review. Ecol Appl. 2020;30(2):e02044 http://dx.doi.org/10.1002/eap.2044.

Delandmeter P, van Sebille E. The Parcels v2.0 Lagrangian framework: new field interpolation schemes. Geosci Model Dev. 2019;12(8):3571–84 http://dx.doi.org/10.5194/gmd-12-3571-2019.

ESA. Land Cover CCI Product User Guide Version 2.0. Tech. Rep. 2017. maps.elie.ucl.ac.be/CCI/viewer/download/ESACCI-LC-Ph2-PUGv2_2.0.pdf.

Everaert G, De Rijcke M, Lonneville B, Janssen CR, Backhaus T, Mees J, et al. Risks of floating microplastic in the global ocean. Environ Pollut. 2020;267(115499):115499 http://dx.doi.org/10.1016/j.envpol.2020.115499.

Geyer R, Jambeck JR, Law KL. Production, use, and fate of all plastics ever made. Sci Adv. 2017;3(7):e1700782 http://dx.doi.org/10.1126/sciadv.1700782.

Ghiggi G, Humphrey V, Seneviratne SI, Gudmundsson L. GRUN: an observation-based global gridded runoff dataset from 1902 to 2014. Earth Syst Sci Data. 2019;11(4):1655–74 http://dx.doi.org/10.5194/essd-11-1655-2019.

Global Wind Atlas 3.0, a free, web-based application developed, owned and operated by the Technical University of Denmark (DTU). The Global Wind Atlas 3.0 is released in partnership with the World Bank Group, utilizing data provided by Vortex, using funding provided by the Energy Sector Management Assistance Program (ESMAP). https://globalwindatlas.info.

Goel MK. Runoff coefficient. In: Encyclopedia of Snow, Ice and Glaciers. Dordrecht: Springer; 2011. p. 952–3. http://dx.doi.org/10.1007/978-90-481-2642-2_456.

Hardesty BD, Harari J, Isobe A, Lebreton L, Maximenko N, Potemra J, et al. Using numerical model simulations to improve the understanding of micro-plastic distribution and pathways in the marine environment. Front Mar Sci. 2017;4 http://dx.doi.org/10.3389/fmars.2017.00030.

Hoellein TJ, Rochman CM. The "plastic cycle": a watershed-scale model of plastic pools and fluxes. Frontiers in Ecology and the Environment. 2021 Apr;19(3):176-83. https://doi.org/10.1002/fee.2294

Jenson SK, Domingue JO. Extracting topographic structure from digital elevation data for geographic information system analysis. American Society for Photogrammetry and Remote Sensing. 1988;54(11):1593–600.

Karamage F, Zhang C, Fang X, Liu T, Ndayisaba F, Nahayo L, et al. Modeling rainfall-runoff response to land use and land cover change in Rwanda (1990–2016). Water (Basel). 2017;9(2):147 http://dx.doi.org/10.3390/w9020147.

Kooi, M., & Koelmans, A. A. (2019). Simplifying microplastic via continuous probability distributions for size, shape, and density. *Environmental Science & Technology Letters*, *6*(9), 551-557.

Lau WWY, Shiran Y, Bailey RM, Cook E, Stuchtey MR, Koskella J, et al. Evaluating scenarios toward zero plastic pollution. Science. 2020;369(6510):1455–61 http://dx.doi.org/10.1126/science.aba9475.

Lebreton LCM, Andrady A. Future scenarios of global plastic waste generation and disposal. Palgrave Commun. 2019;5(1):1–11 http://dx.doi.org/10.1057/s41599-018-0212-7.

Lebreton LCM, Greer SD, Borrero JC. Numerical modelling of floating debris in the world's oceans. Mar Pollut Bull. 2012;64(3):653–61 http://dx.doi.org/10.1016/j.marpolbul.2011.10.027.

Lebreton LCM, van der Zwet J, Damsteeg J-W, Slat B, Andrady A, Reisser J. River plastic emissions to the world's oceans. Nat Commun. 2017;8(1):15611 http://dx.doi.org/10.1038/ncomms15611.

Lehner B, Verdin KL, Jarvis A. New global hydrography derived from spaceborne elevation data. Eos, Transactions, American Geophysical Union. 2008;89(10):93–4 http://dx.doi.org/10.1029/2008EO100001.

Materić D, Kasper-Giebl A, Kau D, Anten M, Greilinger M, Ludewig E, et al. Micro-and Nanoplastics in Alpine Snow: A New Method for Chemical Identification and (Semi) Quantification in the Nanogram Range. Environmental Science & Technology. 2020;54(4):2353–9 http://dx.doi.org/10.1021/acs.est.9b07540.

Maximenko N, Hafner J, Niiler P. Pathways of marine debris derived from trajectories of Lagrangian drifters. Mar Pollut Bull. 2012;65(1–3):51–62 http://dx.doi.org/10.1016/j.marpolbul.2011.04.016.

Meijer LJJ, van Emmerik T, van der Ent R, Schmidt C, Lebreton L. More than 1000 rivers account for 80% of global riverine plastic emissions into the ocean. Sci Adv. 2021;7(18) http://dx.doi.org/10.1126/sciadv.aaz5803

Met Office. National Meteorological Library and Archive Fact sheet 6 – The Beaufort Scale. 2010. https://web.archive.org/web/20121002134429/http://www.metoffice.gov.uk/media/pdf/4/4/Fact_Sheet_No._6_-_Beaufort_Scale.pdf.

Njeru J. The urban political ecology of plastic bag waste problem in Nairobi, Kenya. Geoforum. 2006;37(6):1046–58 http://dx.doi.org/10.1016/j.geoforum.2006.03.003.

Onink, V., Jongedijk, C. E., Hoffman, M. J., van Sebille, E., & Laufkötter, C. (2021). Global simulations of marine plastic transport show plastic trapping in coastal zones. *Environmental Research Letters*, *16*(6), 064053. https://doi.org/10.1088/1748-9326/abecbd

Ribeiro F, Okoffo ED, O'Brien JW, Fraissinet-Tachet S, O'Brien S, Gallen M, et al. Quantitative analysis of selected plastics in high-commercial-value Australian seafood by pyrolysis gas chromatography mass spectrometry. Environ Sci Technol. 2020;54(15):9408–17 http://dx.doi.org/10.1021/acs.est.0c02337.

Royal Netherlands Meteorological Institute (a). Frequentietabellen Windsnelheid in m/s, Distributief in procenten, De Bilt. http://projects.knmi.nl/klimatologie/frequentietabellen/maand.cgi. Accessed 29 May 2020.

Royal Netherlands Meteorological Institute (b). Frequentietabellen Windrichting in graden, Distributief in procenten, De Bilt. http://projects.knmi.nl/klimatologie/frequentietabellen/maand.cgi. Accessed 29 May 2020.

Royal Netherlands Meteorological Institute (c). Daggegevens van het weer in Nederland, RH, Etmaalsom van de neerslag (in 0.1 mm) (-1 voor <0.05 mm). http://projects.knmi.nl/klimatologie/daggegevens/selectie.cgi. Accessed 29 May 2020.

Schmidt C, Krauth T, Wagner S. Export of plastic debris by rivers into the sea. Environ Sci Technol. 2017;51(21):12246–53 http://dx.doi.org/10.1021/acs.est.7b02368.

Schwarz AE, Ligthart TN, Boukris E, van Harmelen T. Sources, transport, and accumulation of different types of plastic litter in aquatic environments: A review study. Mar Pollut Bull. 2019;143:92–100 http://dx.doi.org/10.1016/j.marpolbul.2019.04.029.

ShiChun Z, MeiXia P, HongYa Z, Li D, YongJun T, JianGuo D, et al. Situation and harm of micro-nano plastic pollution in seafood. Journal of Food Safety and Quality. 2019;10(9):2689–96.

Shields A. Application of similarity principles and turbulence research to bed-load movement. 1936.

Sigler M. The effects of plastic pollution on aquatic wildlife: Current situations and future solutions. Water Air Soil Pollut. 2014;225(11) http://dx.doi.org/10.1007/s11270-014-2184-6.

Stephens M. The search for the missing plastic. Phys World. 2020;33(5):40–4 http://dx.doi.org/10.1088/2058-7058/33/5/30.

Syberg K, Palmqvist A, Khan FR, Strand J, Vollertsen J, Clausen LPW, et al. A nationwide assessment of plastic pollution in the Danish realm using citizen science. Sci Rep. 2020;10(1):17773 http://dx.doi.org/10.1038/s41598-020-74768-5.

Tramoy R, Gasperi J, Colasse L, Silvestre M, Dubois P, Noûs C, et al. Transfer dynamics of macroplastics in estuaries – New insights from the Seine estuary: Part 2. Short-term dynamics based on GPS-trackers. Marine Pollution Bulletin. 2020;160:111566 http://dx.doi.org/10.1016/j.marpolbul.2020.111566.

van Emmerik T, Loozen M, van Oeveren K, Buschman F, Prinsen G. Riverine plastic emission from Jakarta into the ocean. Environ Res Lett. 2019;14(8):084033 http://dx.doi.org/10.1088/1748-9326/ab30e8.

van Emmerik T, Mellink Y, Hauk R, Waldschlager K, Schreyers L. Rivers as plastic reservoirs. Front Water. 2022;3 https://www.frontiersin.org/article/10.3389/frwa.2021.786936

van Emmerik T, Schwarz A. Plastic debris in rivers. WIREs Water. 2020. http://dx.doi.org/10.1002/wat2.1398.

van Emmerik T, Vriend P, Roebroek J. An evaluation of the River-OSPAR method for quantifying macrolitter on Dutch riverbanks. Wageningen: Wageningen University. 2020;86 p. http://dx.doi.org/10.18174/519776.

van Sebille E, England MH, Froyland G. Origin, dynamics and evolution of ocean garbage patches from observed surface drifters. Environ Res Lett. 2012;7(4):044040 http://dx.doi.org/10.1088/1748-9326/7/4/044040.

Vethaak AD, Leslie HA. Plastic debris is a human health issue. Environ Sci Technol. 2016;50(13):6825–6 http://dx.doi.org/10.1021/acs.est.6b02569.

Wayman C, Niemann H. The fate of plastic in the ocean environment - a minireview. Environ Sci Process Impacts. 2021 http://dx.doi.org/10.1039/d0em00446d.

Windsor FM, Durance I, Horton AA, Thompson RC, Tyler CR, Ormerod SJ. A catchment-scale perspective of plastic pollution. Glob Chang Biol. 2019;25(4):1207–21 http://dx.doi.org/10.1111/gcb.14572.

Yeo S-S, Hsuan YG. Evaluation of creep behavior of high density polyethylene and polyethylene-terephthalate geogrids. Geotextiles Geomembranes. 2010;28(5):409–21. http://dx.doi.org/10.1016/j.geotexmem.2009.12.003